The cluster species effect on the noble gas cluster interaction with solid surfaces

Nazarov, Anton V.

2021-10

Nazarov , A V , Chernysh , V S , Zavilgelsky , A D , Shemukhin , A A , Lopez-Cazalilla , A , Djurabekova , F & Nordlund , K 2021 , ' The cluster species effect on the noble gas cluster interaction with solid surfaces ' , Surfaces and interfaces , vol. 26 , 101397 . https://doi.org/10.1016/j.surfin.2021.101

http://hdl.handle.net/10138/346941
https://doi.org/10.1016/j.surfin.2021.101397

The cluster species effect on the noble gas cluster interaction with solid surfaces

Anton V. Nazarov , Vladimir S. Chernysh , Andrey D. Zavilgelsky , Andrey A. Shemukhin , Alvaro Lopez-Cazalilla , Flyura Djurabekova , Kai Nordlund

PII: S2468-0230(21)00474-0
DOI: https://doi.org/10.1016/j.surfin.2021.101397
Reference: SURFIN 101397

To appear in: *Surfaces and Interfaces*

Received date: 17 May 2021
Revised date: 30 July 2021
Accepted date: 4 August 2021

Please cite this article as: Anton V. Nazarov , Vladimir S. Chernysh , Andrey D. Zavilgelsky , Andrey A. Shemukhin , Alvaro Lopez-Cazalilla , Flyura Djurabekova , Kai Nordlund , The cluster species effect on the noble gas cluster interaction with solid surfaces, *Surfaces and Interfaces* (2021), doi: https://doi.org/10.1016/j.surfin.2021.101397

The cluster species effect on the noble gas cluster interaction with solid surfaces

Anton V. Nazarov[a,*], Vladimir S. Chernysh[b], Andrey D. Zavilgelsky[b], Andrey A. Shemukhin[a], Alvaro Lopez-Cazalilla[c], Flyura Djurabekova[c,d], Kai Nordlund[c]

[a]Skobeltsyn Institute of Nuclear Physics, Lomonosov Moscow State University, Moscow, 119991 Russia

[b]Physical Faculty, Lomonosov Moscow State University, Moscow 119991, Russia

[c]Department of Physics, University of Helsinki, 00014 Helsinki, Finland

[d]Helsinki Institute of Physics, University of Helsinki, 00014 Helsinki, Finland

*Corresponding author. E-mail address: av.nazarov@physics.msu.ru

Abstract

The effect of noble gas cluster species on the cluster interaction with solid surfaces was investigated. Processes of Ar, Kr and Xe clusters interaction with Cu and Mo surfaces were studied using molecular dynamics simulations. It is shown that lighter cluster front atoms undergo more backscattering from surface atoms, causing more intense multiple collisions between cluster atoms. This affects cluster penetration, energy exchange between the cluster and surface atoms, and cluster thermalization. The influence of energy per cluster atom on these effects is discussed.

Keywords: gas cluster ions, GCIB, surface treatment, molecular dynamics

1. Introduction

Noble gas cluster ion beams (GCIB) is a widely used instrument for surface treatment. Up till now GCIB have demonstrated outstanding polishing and planarization quality by for optics and electronics [1–6]. They can be also used for surface structures fabrication [7–9]. Cluster beams are also used for surface cleaning [10,11] and treatment of biomedical materials [12,13]. Another application of GCIB is material analysis by secondary ion mass spectrometry (SIMS), mostly for organic materials [14–16]. The applicability of GCIB in the mentioned fields is associated with its specific features such as low energy per cluster atom, high energy deposition in a small surface area, high sputtering yield, specific sputtering yield dependence on the impact angle and the angular distributions of sputtered atoms [17–19].

The most used noble gas for GCIB is argon [4,5,8–11,15] due to its easy availability and affordability. However, using different cluster species can affect the cluster – surface interaction process and therefore change the results of the surface treatment. Moreover, the cluster size distribution in the beam differs significantly for different noble gas species [3], so this can be another option to change irradiation parameters.

Studies of the cluster species dependencies may be the key to the optimization of technological processes. Several such studies have been made so far. In Ref. [20] the results of molecular dynamics (MD) simulations of Ar, Ne and Xe cluster impact on Si surface were reported.[20][20] It was shown that the cluster of the same size but consisting of heavier atoms provide higher amount of displacements. The authors explain this effect with the larger momentum of the cluster. The MD simulations have also shown that increasing the mass of the cluster atoms leads to higher transmission of energy to target atoms [21]. Experimental studies [22] have demonstrated that the angular distributions of atoms, sputtered from Cu and W surface, drastically differ for Xe and Ar clusters. Sputtering by Xe clusters demonstrates higher sputtering yields in the direction of the surface normal than Ar clusters. Moreover, it was shown in [23] that for small size clusters (several atoms to several tens of atoms), the cluster atom species also affects the formation of craters and hillocks on the irradiated surface. For SIMS analysis using different noble gases can also affect the fragmentation of sputtered molecules. For

example in [24] it has been shown[24],[24] that using Ar and Xe cluster beams to analyze an insulin film on a silicon substrate results in different spectra in low mass region. However, the intact ion intensities stay mostly the same.

The mentioned above works represent some aspects of cluster species effect on the cluster-surface interaction that are known. However, fundamental studies of cluster species effects are still necessary to thoroughly describe how cluster species affect the gas cluster impact on the solid surface. Such studies can lead to improvement of experimental methods that are used in practical applications of GCIB.

In the current paper, we study the energy exchange between the cluster and surface atoms and the influence of cluster species on this process. The penetration of cluster into the target is considered as well. The simulations of Ar, Kr and Xe clusters impacts on the Cu and Mo surfaces are performed. The common noble gas cluster beam parameters for the applications described above are the following. The cluster size varies from several atoms to thousands and tens of thousands atoms, however, small clusters are often excluded from the beam [1,15,23,25–27]. The beam consisting of clusters with certain size distribution in a wide range of cluster sizes is usually used for practical purposes, however studies with size-selected cluster beams are performed as well [26,28]. The energies per cluster atom vary from several eV to several keV for the mentioned above cases. In current paper we focus on the clusters sizes and energies from this range that is used for practical applications, however some other effects may occur in other size and energy ranges [29,30].

2. Methods

The simulation of GCIB impacts on the Mo and Cu solid surface were simulated with MD method. The PARCAS MD code [31] was used for the simulations. Ar, Kr and Xe cluster ions with the size from 50 to 5000 atoms and the energy of 20 keV were used as projectiles. First, the lattices with the parameters of solid noble gases were generated and then the clusters of required size were cut from these lattices. Such method does not represent the real cluster shape and structure. The shape and structure of noble gas clusters is found to be more complicated, and other complex approach is necessary in

order to simulate it more accurately. Some studies on noble gas cluster shape and structure can be found in [32–35]. However, at the initial stage of impact, the cluster structure is destroyed, and it does not significantly affect the further cluster-surface interaction process.

The targets were Mo and Cu single crystals at room temperature. The incident direction was normal to Mo (100) surface and Cu (111) surface. The lattice preparation and relaxation procedure is described in our previous papers [22].

The simulation cell size is 321×321×107 Å for Mo target and 334×334×113 Å for Cu target and it contains 707,522 and 1,053,100, atoms respectively. Such simulation cell sizes were chosen to be large enough for the energy to dissipate from the interaction area and to avoid any undesired influence from the borders. Periodic boundary conditions were applied in the *x* and *y* lateral directions to simulate bulk target. Three bottom atomic layers in the *z* direction were fixed to prevent the simulation cell motion. Berendsen thermal bath [36] was applied at the borders to let the heat leave the simulation cell. The simulated time varied from 10 to 20 ps depending on the cluster size and species.

The Lennard–Jones potentials were used to describe the interaction between noble gas atoms [37,38]. For the Mo-Mo and Cu-Cu interactions, embedded atom method (EAM) potentials were used [39,40]. Such potentials have shown good reliability describing the properties of metals [37,39,41]. The Ziegler–Biersack–Littmark (ZBL) [42] universal repulsive potential is used to describe the Ar–Mo, Ar–Cu, Kr–Mo, Kr–Cu, Xe–Mo and Xe–Cu interactions. These potentials are often used for simulations of atomic collisions [20,38,43–46]. The use of these kind of potentials will be discussed below.

The simulations were carried out using “Lomonosov-2” supercomputer facility at Moscow State University [47]. The OVITO software [48] was used to visualize the simulation results.

3. Results and discussion

The snapshots of 20 keV Ar_{500}, Kr_{500} and Xe_{500} cluster impacts on Mo surface are presented in Fig.1. The arrows represent the velocities of cluster atoms. The velocities are shown only for atoms with $V_z < 0$ (directed against the target surface). To show this

process in dynamics, the animations are included in the supplementary materials. It is clearly seen that for Xe atoms most of the momenta are directed into the target, however for Ar atoms most of the atoms have momentum turned to the direction from the target surface. This effect can be easily understood from simple kinematics. It is well known that heavier atoms cannot scatter back from the lighter ones, and there is a maximum scattering angle that depends on the target and projectile atom mass ratio [49].

When the front atoms of the Ar cluster hit the surface, a large amount of these atoms are scattered back. This initiates numerous collisions of cluster atoms with each other from the very beginning of the impact. In case of Xe atoms that are heavier than target atoms, the front atoms are scattered at smaller angles, so cluster atoms keep their initial direction during the longer path, the stopping of incoming atoms is lower – the so-called clearing-the-way effect [50,51]. Thus, the mass ratio of cluster and target atoms affect how cluster atoms can reach target surface and penetrate inside it. The projected ranges distributions for the atoms of the mentioned above clusters are presented in Fig.2. The zero coordinate marked with a vertical line on the plots corresponds to the target surface. The positive direction is directed into the target. It is noticeable that for Ar cluster a much larger amount (41%) of atoms does not even reach the target surface in comparison to Kr and Xe clusters (26% and 25% respectively).

One could expect that for the cluster, consisting of Kr atoms, that are lighter than the target Mo atoms, the results should be closer to the case of Ar than of Xe, however the opposite is observed. The analysis of the scattering cross-sections is necessary to explain this inconsistency. The differential cross sections for 40 eV Ar, Kr and Xe atoms scattering on Mo atoms for used ZBL potentials are presented in Fig.3. The energy of 40 eV per atom corresponds to 20 keV cluster of 500 atoms. Calculated from these cross sections, the probability of scattering at angles higher than 90 degrees for Kr is almost 10 times lower than for Ar. Thus, Kr cluster atoms remain closer to their initial direction in the first phase of the impact and the clearing-the-way effect is more pronounced.

It is known, that as a result of the impact the cluster gets thermalized [52], and the extent of the thermalization depends on the energy per atom. To study the cluster thermalization dependence on the cluster atom species the velocity distributions of cluster atoms at the end of the impact are analyzed. These distributions are presented in

Fig. 4. The Maxwell-Boltzmann distributions corresponding to the average velocity for each case are plotted with the calculated distributions.

As seen from the distributions, the Ar clusters are more thermalized than Xe clusters with the same energy and cluster size, especially for lower energy per atom. This effect also could be explained by the backscattering of lighter Ar atoms from heavy Mo target atoms what results in more intense cluster atoms collisions with each other. These collisions for their part lead to the thermalization of the cluster. We should point out that clusters with low energy per atom demonstrate very incomplete thermalization. Such cluster atoms do not penetrate the target due to insufficient energy. In this case the cluster is being strongly compressed on the surface (Fig. 5). As a result of this compression, the cluster collapses and most atoms get lateral momentum. The amount of collisions between cluster atoms is low that leads to incomplete thermalization of cluster atoms. However, better thermalization of argon cluster is observed even for a cluster consisting of 5000 atoms, what corresponds to 4 eV per atom.

The other characteristic that is influenced by the cluster species is the energy transferred from cluster to target atoms. Fig. 6 represents the time dependence of the total energy of cluster atoms during the impact for 20 keV Ar_{500}, Kr_{500} and Xe_{500} clusters impacting Mo and Cu surfaces. The first points on the curves correspond to the moment, when the cluster reaches the surface, then the total cluster energy starts to decrease due to the energy transfer to target atoms. At large times the energy transfer process is finished and the total energy of the scattered cluster atoms becomes constant.

The first thing to point out is that the energy transfer rate is lower for the heavier cluster atoms. This is because heavier atoms are slower and when the front atoms have already hit the surface it takes more time for the following atoms to reach the interaction area. Moreover, due to clearing-the-way effect, the atoms from the heavier cluster can penetrate deeper into the target without losing energy.

The amount of transferred energy also depends on the cluster species. It is seen from Fig.6 that Xe transfers the largest amount of energy and Ar the smallest amount of energy for both cases of Mo and Cu targets. We should note that the maximum amount of energy transferred in the individual collision (Table 1) is higher for Ar than for Xe in case of Cu target and the opposite in case of Mo target, however it does not affect the ratio of the

energy transmitted by different clusters in these two cases. Therefore, the kinematics of the single collisions of cluster and target atoms is not responsible for the difference in the transmitted energy.

This difference is caused by the backscattering of lighter atoms from heavier target atoms that lead to multiple collisions in the lighter cluster that makes cluster atoms to carry away more energy. The heavier cluster atoms scatter mostly in forward direction and let the incoming atoms transfer more energy.

The ratio of energy transferred to the target atoms for different cluster sizes is presented in Fig. 7. The transferred energy ratio is plotted over the energy per cluster atom as it was shown that this parameter can be universal for both changing the cluster size and energy [21]. The difference in transferred energy mentioned above for different cluster species is observed in a certain range of E/n (E – initial energy of cluster and n – the number of atoms that make up the cluster). The cluster with high energy per atom fully penetrates the target. The cluster atoms in this case collide with a number of target atoms and transmit most of their energy in these collisions. Hence, the collisions between cluster atoms do not affect the energy transfer in this case.

The atoms of clusters with the E/n in the medium range partly penetrate the target and the collisions between cluster atoms start to play a considerable role. For this case, the effect of the cluster species described above is significant.

On the other hand, the cluster with low energy per atom does not penetrate the target just causing a slight deformation of the surface that would be relaxed after the impact. In this case the cluster compression described above takes place (Fig.5). During this compression, many atoms on the outer part of the cluster change their direction along the surface almost without losing energy, so these atoms do not take part in energy transmission to the surface. Moreover, the compression process for the atoms from the center of the cluster is not that much affected by the front atoms scattered from the target atoms. So the influence mass ratio of cluster and target atom has low influence on the energy transmission in this case.

We should note that all presented results are obtained in simulations with ZBL potentials used for the interactions between the cluster and target atoms. These are

screened Coulomb potentials and such potentials are widely used to describe the atomic collisions [20,38,43–46]. The ZBL potentials are repulsive with no attractive part. In the current work these potentials fit well to study the effect of cluster species on the kinematics of the cluster – surface interaction. However, considering the attraction in the interaction between cluster and target atoms, can lead to more effects of cluster species or amend the effects discussed in current paper, especially for Xe [53], for which the potentials with an attractive part can be found [54,55]. Moreover, the electronic stopping is not taken into account, however in [56] it was shown that it can also affect the simulation results, and the electronic stopping power strongly depends on the projectile species and energies. Such simulations are the topic of future work.

4. Conclusions

Using MD simulations of Ar, Kr and Xe cluster impacts on Mo and Cu surface the cluster species effects have been studied. The mass ratio of cluster and target atoms affects the scattering of the front cluster atoms that hit the surface first. Due to that, a large number of collisions between cluster atoms occur in the lighter cluster. This leads to shallower penetration of cluster atoms into the target, better thermalization of the lighter cluster at the end of the impact, and less energy transfer to the target. The energy transfer rate is lower for the heavier cluster due to its lower velocity and more pronounced clearing-the-way effect. The effect on transferred energy value is significant only in a certain range of cluster *E/n*, however the effect on the cluster thermalization is observed in a wider energy per atom range.

Acknowledgements

The research is carried out using the equipment of the shared research facilities of HPC computing resources at Lomonosov Moscow State University.

The results on the cluster penetration and energy transfer were obtained within the Russian Science Foundation grant [project № 20-72-10118]. The results on cluster thermalization were obtained within the Russian Science Foundation grant [project № 21-19-00310].

The research was partly carried out using the equipment of MIPT nuclear physics facility.

Declaration of interests

The authors declare the following financial interests/personal relationships which may be considered as potential competing interests

CRediT authorship contribution statement

A.A. Nazarov: Conceptualization, Investigation, Visualization, Writing - original draft.

A.D. Zavilgelsky: Investigation, Visualization.

V.S. Chernysh: Conceptualization, Supervision, Writing - review & editing, Funding Acquisition.

A.A. Shemukhin: Funding Acquisition.

Alvaro Lopez-Cazalilla, Kai Nordlund, Flyura Djurabekova: Software, Writing - review & editing.

References

[1] T. Hirota, N. Toyoda, A. Yamamoto, I. Yamada, Modification and smoothing of patterned surface by gas cluster ion beam irradiation, Appl. Surf. Sci. 256 (2009) 1110–1113. https://doi.org/10.1016/j.apsusc.2009.05.166.

[2] Z. Insepov, A. Hassanein, J. Norem, D.R. Swenson, Advanced surface polishing using gas cluster ion beams, Nucl. Instruments Methods Phys. Res. Sect. B Beam Interact. with Mater. Atoms. 261 (2007) 664–668. https://doi.org/10.1016/j.nimb.2007.04.134.

[3] A.E. Ieshkin, D.S. Kireev, Y.A. Ermakov, A.S. Trifonov, D.E. Presnov, A. V. Garshev, Y. V. Anufriev, I.G. Prokhorova, V.A. Krupenin, V.S. Chernysh, The quantitative analysis of silicon carbide surface smoothing by Ar and Xe cluster ions, Nucl. Instruments Methods Phys. Res. Sect. B Beam Interact. with Mater. Atoms. 421 (2018) 27–31. https://doi.org/10.1016/j.nimb.2018.02.019.

[4] N. Toyoda, T. Hirota, I. Yamada, H. Yakushiji, T. Hinoue, T. Ono, H. Matsumoto, Fabrication of planarized discrete track media using gas cluster ion beams, IEEE Trans. Magn. 46 (2010) 1599–1602. https://doi.org/10.1109/TMAG.2010.2048748.

[5] A. Ieshkin, D. Kireev, V. Chernysh, A. Molchanov, A. Serebryakov, M. Chirkin, Decomposition of AFM images of ultrasmooth optical surface polished with gas cluster ion beam, Surf. Topogr. Metrol. Prop. 7 (2019). https://doi.org/10.1088/2051-672X/ab1f49.

[6] A.E. Ieshkin, K.D. Kushkina, D.S. Kireev, Y.A. Ermakov, V.S. Chernysh, Polishing superhard material surfaces with gas-cluster ion beams, Tech. Phys. Lett. 43 (2017) 95–97. https://doi.org/10.1134/S1063785017010205.

[7] N. Toyoda, T. Mashita, I. Yamada, Nano structure formation by gas cluster ion beam irradiations at oblique incidence, Nucl. Instruments Methods Phys. Res. Sect. B Beam Interact. with Mater. Atoms. 232 (2005) 212–216. https://doi.org/10.1016/j.nimb.2005.03.047.

[8] N. Toyoda, B. Tilakaratne, I. Saleem, W.K. Chu, Cluster beams, nano-ripples, and bio applications, Appl. Phys. Rev. 6 (2019). https://doi.org/10.1063/1.5030500.

[9] [illegible] cluster ion beam on copper surface at elevated temperatures, Mater. Lett. 272 (2020) 127829. https://doi.org/10.1016/j.matlet.2020.127829.

[10] M. Tiddia, M.P. Seah, A.G. Shard, G. Mula, R. Havelund, I.S. Gilmore, Argon cluster cleaning of Ga+ FIB-milled sections of organic and hybrid materials, Surf. Interface Anal. 52 (2020) 327–334. https://doi.org/10.1002/sia.6522.

[11] D.J. Yun, S.Y. Kim, D.S. Ko, S. Heo, K.H. Kim, S.H. Kim, Simple and effective cleaning method for RuO2 nanosheet films for flexible transparent conducting electrodes, Appl. Surf. Sci. 529 (2020) 147154. https://doi.org/10.1016/j.apsusc.2020.147154.

[12] Y. Uozumi, N. Toyoda, I. Yamada, Surface Modification of PEEK with Gas Cluster Ion Beam Irradiation, Proc. Int. Conf. Ion Implant. Technol. (2017) 9–11. https://doi.org/10.1109/IIT.2016.7882911.

[13] A. Kirkpatrick, S. Kirkpatrick, M. Walsh, S. Chau, M. Mack, S. Harrison, R. Svrluga, J. Khoury, Investigation of accelerated neutral atom beams created from gas cluster ion beams, Nucl. Instruments Methods Phys. Res. Sect. B Beam Interact. with Mater. Atoms. 307 (2013) 281–289. https://doi.org/10.1016/j.nimb.2012.11.084.

[14] M. Finšgar, Advanced surface analysis using GCIB-C60++-tandem-ToF-SIMS and GCIB-XPS of 2-mercaptobenzimidazole corrosion inhibitor on brass, Microchem. J. 159 (2020). https://doi.org/10.1016/j.microc.2020.105495.

[15] V. Cristaudo, C. Poleunis, P. Laha, P. Eloy, T. Hauffman, H. Terryn, A. Delcorte, Ion yield enhancement at the organic/inorganic interface in SIMS analysis using Ar-GCIB, Appl. Surf. Sci. 536 (2021) 147716. https://doi.org/10.1016/j.apsusc.2020.147716.

[16] A. Delcorte, V. Delmez, C. Dupont-Gillain, C. Lauzin, H. Jefford, M. Chundak, C. Poleunis, K. Moshkunov, Large cluster ions: Soft local probes and tools for organic and bio surfaces, Phys. Chem. Chem. Phys. 22 (2020) 17427–17447. https://doi.org/10.1039/d0cp02398a.

[17] V.N. Popok, I. Barke, E.E.B. Campbell, K.-H. Meiwes-Broer, Cluster-surface interaction: From soft landing to implantation, Surf. Sci. Rep. 66 (2011) 347–377. https://doi.org/10.1016/j.surfrep.2011.05.002.

[18] A.E. Ieshkin, A.V. Nazarov, A.A. Tatarintsev, D.S. Kireev, A.D. Zavilgelsky, A.A. Shemukhin, V.S. Chernysh, Energy distributions of the particles sputtered by gas cluster ions. Experiment and computer simulation, Surf. Coatings Technol. 404 (2020) 126505.

[19] N. Toyoda, I. Yamada, Gas cluster ion beam equipment and applications for surface processing, IEEE Trans. Plasma Sci. 36 (2008) 1471–1488. https://doi.org/10.1109/TPS.2008.927266.

[20] T. Aoki, J. Matsuo, G. Takaoka, I. Yamada, Cluster species and cluster size dependence of damage formation by cluster ion impact, Nucl. Instruments Methods Phys. Res. Sect. B Beam Interact. with Mater. Atoms. 206 (2003) 861–865. https://doi.org/10.1016/S0168-583X(03)00879-6.

[21] R.J. Paruch, Z. Postawa, B.J. Garrison, Physical basis of energy per cluster atom in the universal concept of sputtering, J. Vac. Sci. Technol. B, Nanotechnol. Microelectron. Mater. Process. Meas. Phenom. 34 (2016) 03H105. https://doi.org/10.1116/1.4940153.

[22] V.S. Chernysh, A.E. Ieshkin, D.S. Kireev, A.V. Nazarov, A.D. Zavilgelsky, Interaction of gas cluster ions with solids: Experiment and computer simulations, Surf. Coatings Technol. 388 (2020) 125608. https://doi.org/10.1016/j.surfcoat.2020.125608.

[23] S. Prasalovich, V. Popok, P. Persson, E.E.B. Campbell, Experimental studies of complex crater formation under cluster implantation of solids, Eur. Phys. J. D. 36 (2005) 79–88. https://doi.org/10.1140/epjd/e2005-00197-2.

[24] K. Moritani, M. Kanai, K. Goto, I. Ihara, N. Inui, K. Mochiji, Secondary ion emission from insulin film bombarded with methane and noble gas cluster ion beams, Nucl. Instruments Methods Phys. Res. Sect. B Beam Interact. with Mater. Atoms. 315 (2013) 300–303. https://doi.org/10.1016/j.nimb.2013.05.064.

[25] J. Matsuo, S. Nishiyama, T. Aoki, T. Seki, Size effect in cluster collision on solid surfaces, Nucl. Instruments Methods Phys. Res. Sect. B Beam Interact. with Mater. Atoms. 257 (2007) 627–631. https://doi.org/10.1016/j.nimb.2007.01.164.

[26] K. Moritani, G. Mukai, M. Hashinokuchi, K. Mochiji, Energy-dependent fragmentation of polystyrene molecule using size-selected Ar gas cluster ion beam projectile, Surf. Interface Anal. 43 (2011) 241–244. https://doi.org/10.1002/sia.3551.

[27] A.A. Andreev, V.S. Chernysh, Y.A. Ermakov, A.E. Ieshkin, Design and investigation of gas cluster ion accelerator, Vacuum. 91 (2013) 47–53. https://doi.org/10.1016/j.vacuum.2012.11.001.

[28] K. Nakamura, S. Houzumi, N. Toyoda, K. Mochiji, T. Mitamura, I. Yamada, Cluster size dependences of bombardment effects using mass-selected gas cluster ion beams, Nucl. Instruments Methods Phys. Res. Sect. B Beam Interact. with Mater. Atoms. 261 (2007) 660–663. https://doi.org/10.1016/j.nimb.2007.04.268.

[29] J. Samela, K. Nordlund, Atomistic simulation of the transition from atomistic to macroscopic cratering, Phys. Rev. Lett. 101 (2008) 1–4. https://doi.org/10.1103/PhysRevLett.101.027601.

[30] J. Samela, K. Nordlund, Classical molecular dynamics simulations of hypervelocity nanoparticle impacts on amorphous silica, Phys. Rev. B - Condens. Matter Mater. Phys. 81 (2010) 1–5. https://doi.org/10.1103/PhysRevB.81.054108.

[31] K. Nordlund, Molecular dynamics simulation of ion ranges in the 1-100 keV energy range, Comput. Mater. Sci. 3 (1995) 448–456. https://doi.org/10.1016/0927-0256(94)00085-Q.

[32] I.A. Harris, K.A. Norman, R.V. Mulkern, J.A. Northby, Icosahedral structure of large charged argon clusters, Chem. Phys. Lett. 130 (1986) 316–320.

[33] S.I. Kovalenko, D.D. Solnyshkin, E.A. Bondarenko, E.T. Verkhovtseva, Electron diffraction study of crystal phase appearance in rare-gases and nitrogen clusters, Izv. Akad. Nauk. Ser. Fiz. 62 (1998) 1107–1112.

[34] B.W. van De Waal, G. Torchet, M.F. De Feraudy, Structure of large argon clusters ArN, $10^3<N<10^5$: Experiments and simulations, Chem. Phys. Lett. 331 (2000) 57–63. https://doi.org/10.1016/S0009-2614(00)01050-2.

[35] W. Miehle, O. Kandier, T. Leisner, O. Echt, Mass spectrometric evidence for icosahedral structure in large rare gas clusters: Ar, Kr, Xe, J. Chem. Phys. 91 (1989) 5940–5952. https://doi.org/10.1063/1.457464.

[36] H.J.C. Berendsen, J.P.M. Postma, W.F. Van Gunsteren, A. Dinola, J.R. Haak, Molecular dynamics with coupling to an external bath, J. Chem. Phys. 81 (1984) 3684–3690. https://doi.org/10.1063/1.448118.

[37] C. Anders, G. Ziegenhain, S. Zimmermann, H.M. Urbassek, Nuclear Instruments and Methods in Physics Research B Cluster-induced crater formation, Nucl. Inst. Methods Phys. Res. B. 267 (2009) 3122–3125. https://doi.org/10.1016/j.nimb.2009.07.002.

[38] V. V. Sirotkin, Molecular-Dynamics Simulation of the Interaction of Argon Cluster Ions with Titanium Surface, J. Surf. Investig. 14 (2020) 292–297. https://doi.org/10.1134/S1027451020020342.

[39] E. Salonen, T. Järvi, K. Nordlund, J. Keinonen, Effects of the surface structure and cluster bombardment on the self-sputtering of molybdenum, J. Phys. Condens. Matter. 15 (2003) 5845–5855. https://doi.org/10.1088/0953-8984/15/34/314.

[40] M.J. Sabochick, N.Q. Lam, Radiation-induced amorphization of ordered intermetallic compounds CuTi, CuTi2, and Cu4Ti3: A molecular-dynamics study, Phys. Rev. B. 43 (1991) 5243–5252. https://doi.org/10.1103/PhysRevB.43.5243.

[41] D. Maciazek, M. Kanski, L. Gaza, B.J. Garrison, Z. Postawa, Computer modeling of angular emission from Ag(100) and Mo(100) surfaces due to Ar n cluster bombardment , J. Vac. Sci. Technol. B, Nanotechnol. Microelectron. Mater. Process. Meas. Phenom. 34 (2016) 03H114. https://doi.org/10.1116/1.4942202.

[42] J.F. Ziegler, M.D. Ziegler, J.P. Biersack, SRIM - The stopping and range of ions in matter (2010), Nucl. Instruments Methods Phys. Res. Sect. B Beam Interact. with Mater. Atoms. 268 (2010) 1818–1823. https://doi.org/10.1016/j.nimb.2010.02.091.

[43] T. Aoki, T. Seki, S. Ninomiya, T. Matsuo, Study of crater formation and sputtering process with large gas cluster impact by molecular dynamics simulations, Nucl. Instruments Methods Phys. Res. Sect. B Beam Interact. with Mater. Atoms. 267 (2009) 1424–1427. https://doi.org/10.1016/j.nimb.2009.01.162.

[44] V. V. Sirotkin, Molecular Dynamics Study of the Interaction of Accelerated Argon Atoms with a Pyrolytic Carbon Surface, Bull. Russ. Acad. Sci. Phys. 84 (2020) 693–697. https://doi.org/10.3103/S1062873820060258.

[45] N.G. Korobeishchikov, P. V. Stishenko, Y.A. Popenko, M.A. Roenko, I. V. Nikolaev, Interaction of accelerated argon cluster ions with a silicon dioxide surface, AIP Conf. Proc. 1876 (2017). https://doi.org/10.1063/1.4998884.

[46] D. MacIążek, M. Kański, Z. Postawa, Intuitive Model of Surface Modification Induced by Cluster Ion Beams, Anal. Chem. 92 (2020) 7349–7353. https://doi.org/10.1021/acs.analchem.0c01219.

[47] V.. Sadovnichy, A.. Tikhonravov, V.. Voevodin, " Lomonosov": Supercomputing at Moscow State University, Contemp. High Perform. Comput. From Petascale Towar. Exascale. (2013) 283–307. http://refhub.elsevier.com/S0257-8972(20)31174-9/rf0190.

[48] A. Stukowski, Visualization and analysis of atomistic simulation data with OVITO-the Open Visualization Tool, Model. Simul. Mater. Sci. Eng. 18 (2010). https://doi.org/10.1088/0965-0393/18/1/015012.

[49] L.C. Feldman, J.W. Mayer, Fundamentals of Surface and Thin Film Analysis, Pearson, 1986.

[50] V.I. Shulga, P. Sigmund, Penetration of slow gold clusters through silicon, Nucl. Inst. Methods Phys. Res. B. 47 (1990) 236–242. https://doi.org/10.1016/0168-583X(90)90751-F.

[51] V.I. Shulga, P. Sigmund, Interaction of slow (100 eV/atom) copper clusters with thin gold films: reflection, transmission, and sputtering at normal and oblique incidence, Nucl. Inst. Methods Phys. Res. B. 62 (1991) 23–34. https://doi.org/10.1016/0168-583X(91)95923-2.

[52] I. Arias, Molecular Dynamics Simulation of Cluster Ion Impact on Solid Surfaces, 2000. http://hdl.handle.net/2433/8942.

[53] J. Haner, G.J. Schrobilgen, The chemistry of Xenon(IV), Chem. Rev. 115 (2015) 1255–1295. https://doi.org/10.1021/cr500427p.

[54] S. V. Starikov, Z. Insepov, J. Rest, A.Y. Kuksin, G.E. Norman, V. V. Stegailov, A. V. Yanilkin, Radiation-induced damage and evolution of defects in Mo, Phys. Rev. B - Condens. Matter Mater. Phys. 84 (2011) 1–8. https://doi.org/10.1103/PhysRevB.84.104109.

[55] D.E. Smirnova, A.Y. Kuksin, S. V. Starikov, V. V. Stegailov, Z. Insepov, J. Rest, A.M. Yacout, A ternary EAM interatomic potential for U-Mo alloys with xenon, Model. Simul. Mater. Sci. Eng. 21 (2013). https://doi.org/10.1088/0965-0393/21/3/035011.

[56] J. Tian, W. Zhou, Q. Feng, J. Zheng, Molecular dynamics simulations with electronic stopping can reproduce experimental sputtering yields of metals impacted by large cluster ions, Appl. Surf. Sci. 435 (2018) 65–71. https://doi.org/10.1016/j.apsusc.2017.11.080.

Captions

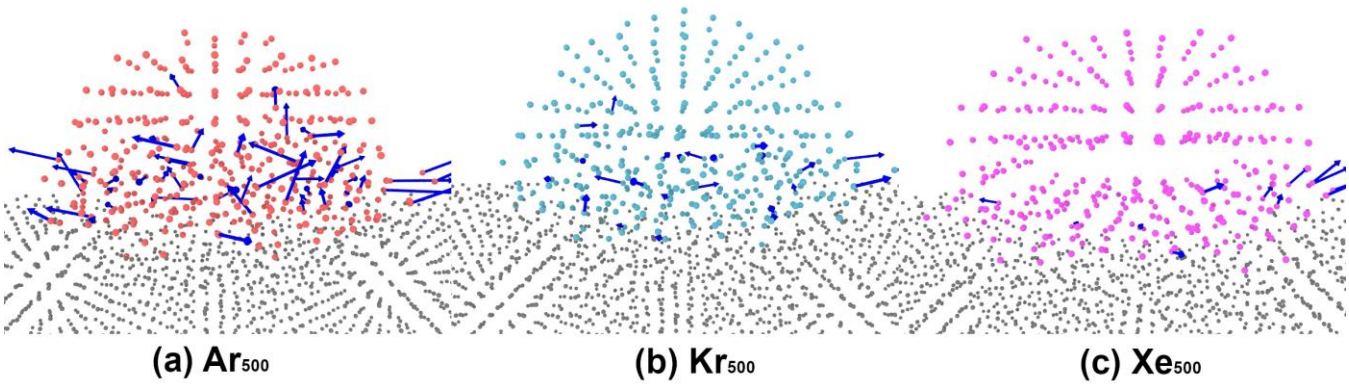

Fig. 1. Snapshots of 20 keV Ar_{500} (a), Kr_{500} (b), and Xe_{500} (c) cluster impacts on Mo surface. The time from the beginning of the impact is 110 fs (a), 160 fs (b), and 200 fs (c). The time from the beginning of the impact for each snapshot is inversely proportional to the cluster velocity. The arrows represent the velocities for cluster atoms with $V_z < 0$ (directed against the target surface).

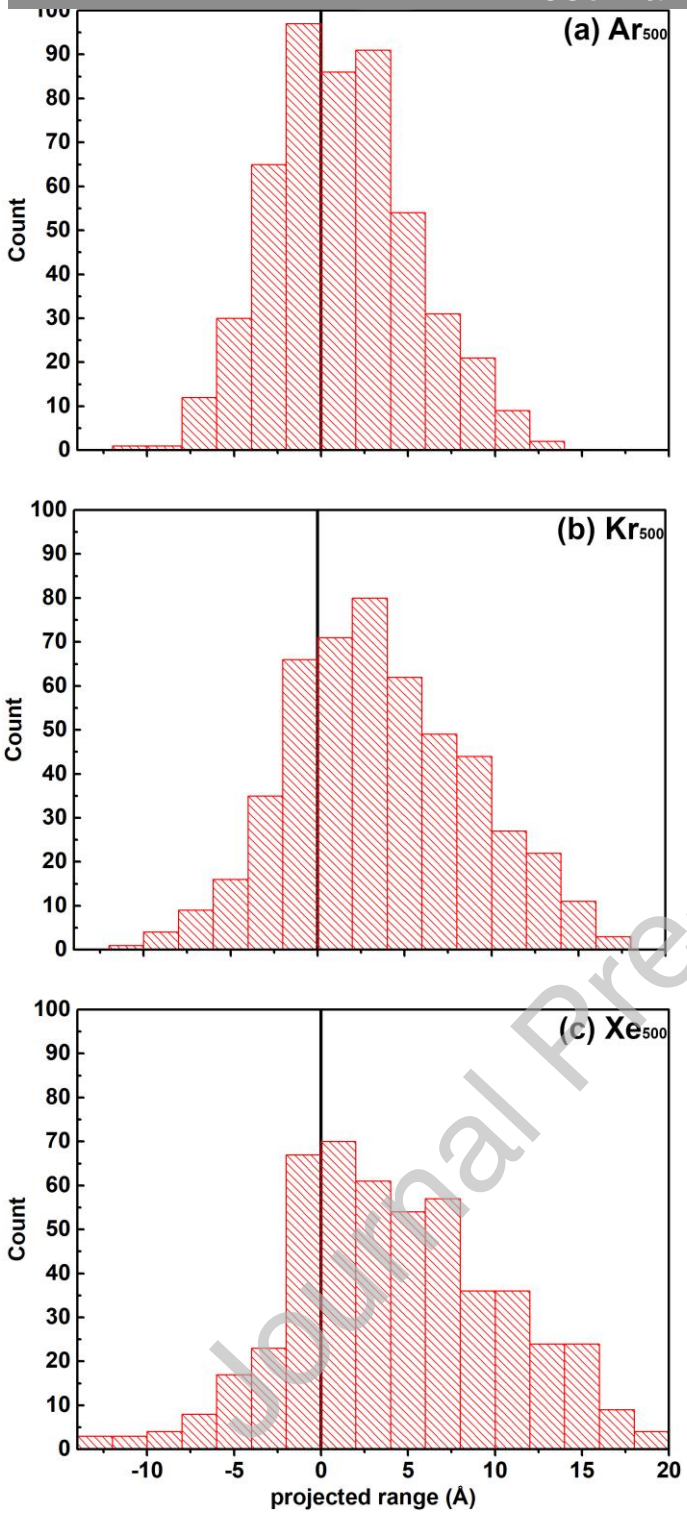

Fig. 2. Projected range distributions for the 20 keV Ar_{500} (a), Kr_{500} (b), and Xe_{500} (c) cluster atoms impacting Mo target. Black vertical line represents target surface.

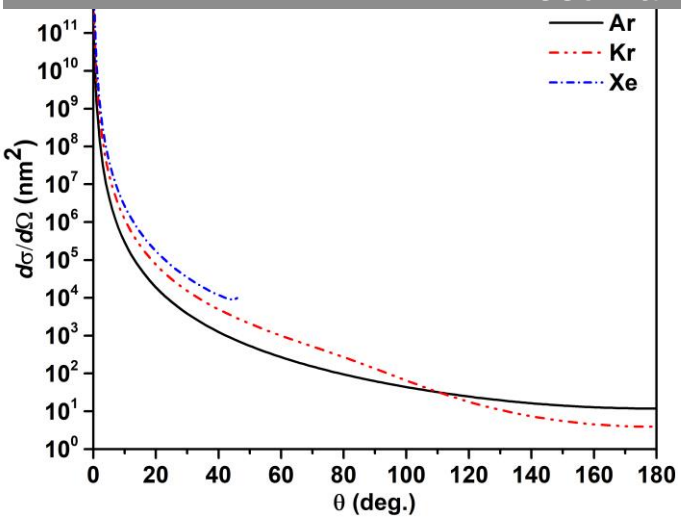

Fig. 3. Differential cross sections for Ar, Kr and Xe atoms with 40 eV kinetic energy scattering on Mo atoms, using ZBL potentials.

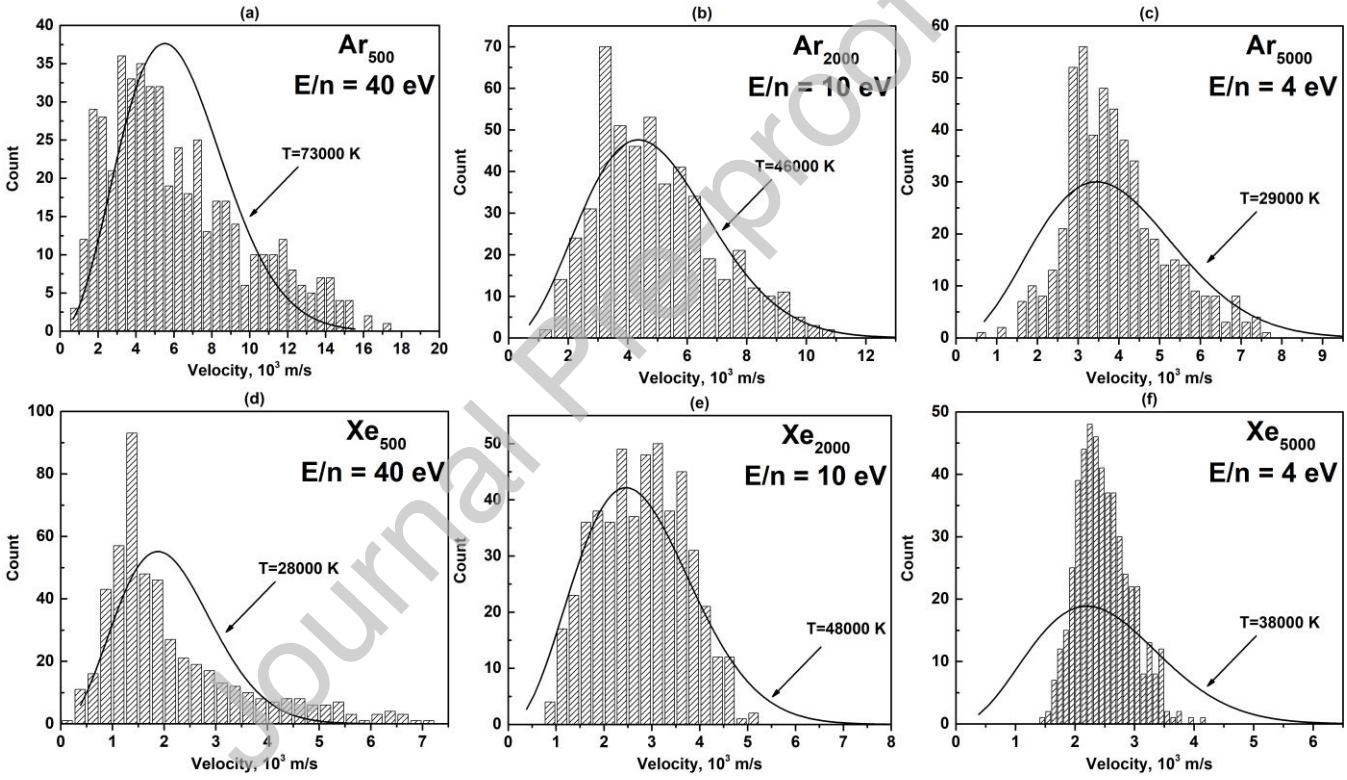

Fig. 4. Velocity distributions of 20 keV Ar_{500} (a), Ar_{2000} (b), Ar_{5000} (c), Xe_{500} (d), Xe_{2000} (e), Xe_{5000} (f) cluster atoms in the end of the impact and Maxwell-Boltzmann distributions corresponding to the average velocity.

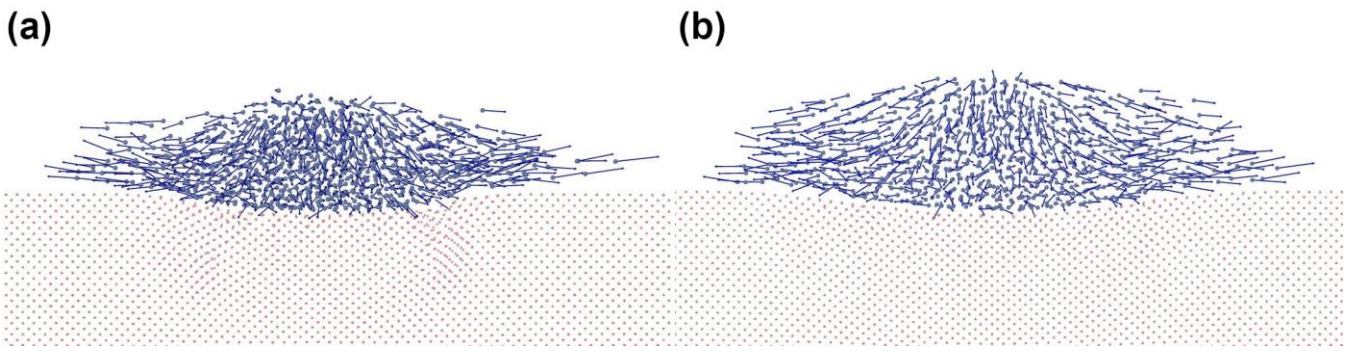

Fig.5. Snapshots of Ar_{5000} (a) and Xe_{5000} (b) impacts on Mo surface. The arrows represent the directions of the atoms velocities. The time from the beginning of the impact for each snapshot is in inverse ratio to the cluster velocity.

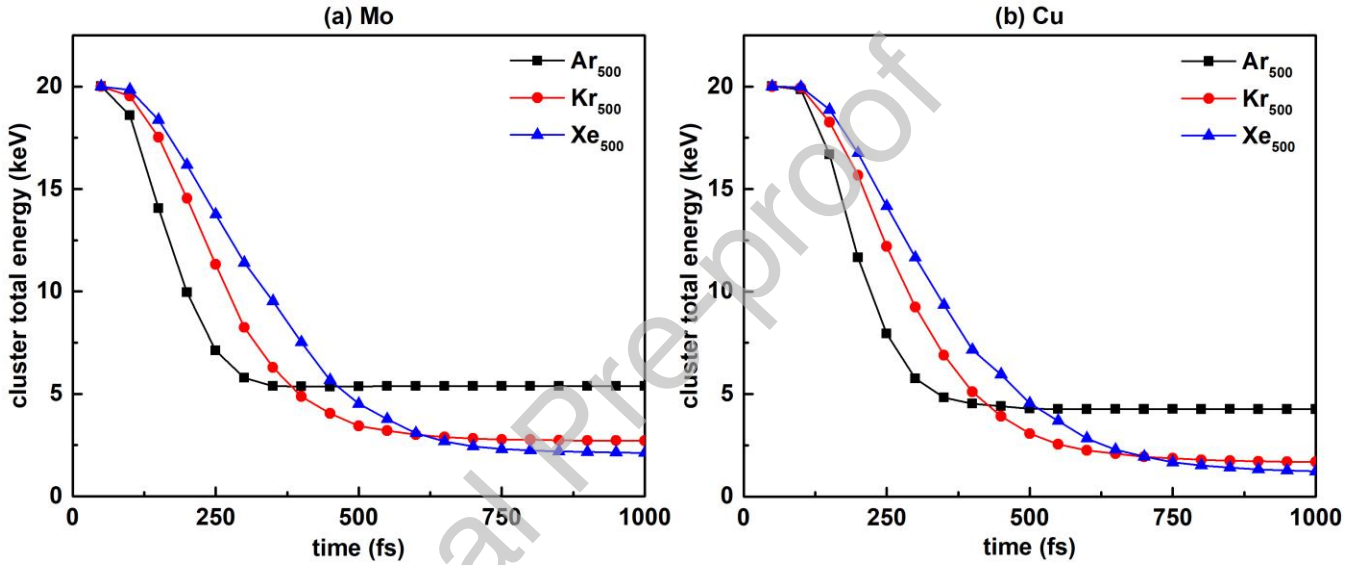

Fig. 6. Time dependence of the total energy of cluster atoms during the impact for 20 keV Ar_{500}, Kr_{500} and Xe_{500} clusters, impacting Mo (a) and Cu (b) surfaces.

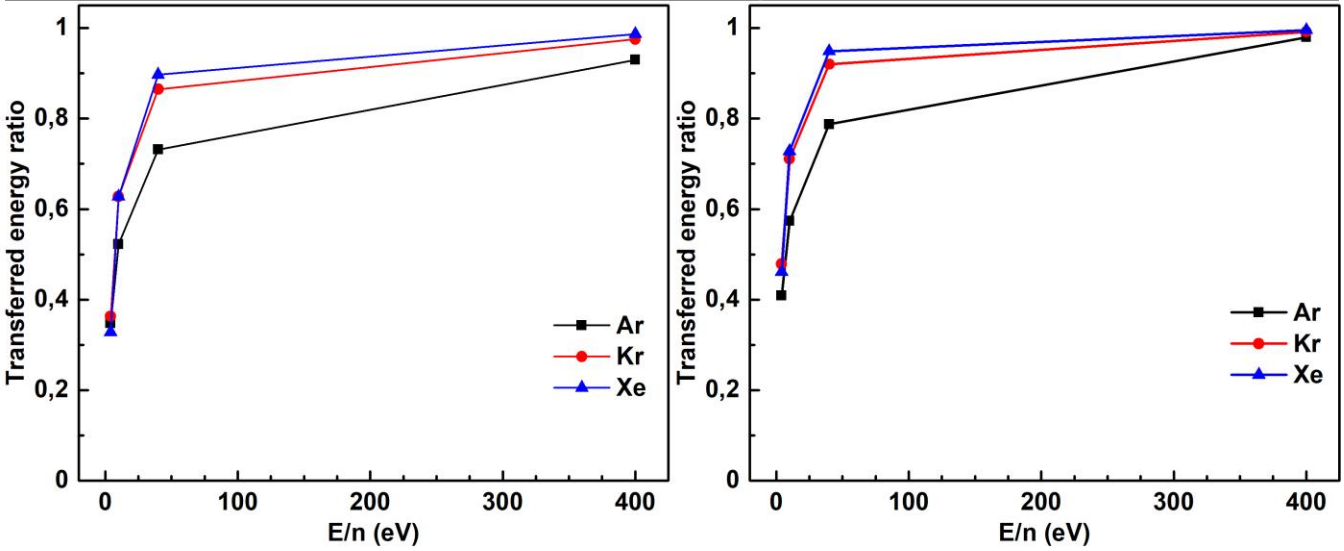

Fig. 7. The E/n dependence of the transferred energy ratio for Ar, Kr and Xe clusters impacting Mo (a) and Cu (b) targets.

Table 1. Maximal kinematic factor for different species of impacting and target atoms.

	Cu	**Mo**
Ar	0,948	0,830
Kr	0,981	0,996
Xe	0,880	0,976